nature geoscience

SEPTEMBER 2010 VOL 3 NO 9
www.nature.com/naturegeoscience

Remains of pre-Marinoan sponges?

OCEAN EDDIES
Dispersed in the west

METHANOGENS IN MOSS
A global relationship

BIRTH OF THE SOLAR SYSTEM
Earlier than assumed

nature geoscience

ARTICLES

PUBLISHED ONLINE: 17 AUGUST 2010 | DOI: 10.1038/NGEO934

Possible animal-body fossils in pre-Marinoan limestones from South Australia

Adam C. Maloof[1]*, Catherine V. Rose[1], Robert Beach[2], Bradley M. Samuels[2], Claire C. Calmet[1], Douglas H. Erwin[3], Gerald R. Poirier[4], Nan Yao[4] and Frederik J. Simons[1]

The Neoproterozoic era was punctuated by the Sturtian (about 710 million years ago) and Marinoan (about 635 million years ago) intervals of glaciation. In South Australia, the rocks left behind by the glaciations are separated by a succession of limestones and shales, which were deposited at tropical latitudes. Here we describe millimetre- to centimetre-scale fossils from the Trezona Formation, which pre-dates the Marinoan glaciation. These weakly calcified fossils occur as anvil, wishbone, ring and perforated slab shapes and are contained within stromatolitic limestones. The Trezona Formation fossils pre-date the oldest known calcified fossils of this size by 90 million years, and cannot be separated from the surrounding calcite matrix or imaged by traditional X-ray-based tomographic scanning methods. Instead, we have traced cross-sections of individual fossils by serially grinding and scanning each sample at a resolution of 50.8 μm. From these images we constructed three-dimensional digital models of the fossils. Our reconstructions show a population of ellipsoidal organisms without symmetry and with a network of interior canals that lead to circular apertures on the fossil surface. We suggest that several characteristics of these reef-dwelling fossils are best explained if the fossils are identified as sponge-grade metazoans.

Geologic setting

The older of two Cryogenian glacial intervals in South Australia (Fig. 1a,b) is known as the Sturtian and is composed of Yudnamutana subgroup diamictites, siltstones and banded iron formations[1]. A sensitive high-resolution ion microprobe (SHRIMP) U–Pb zircon age of 659.7 ± 5.3 Myr from a tuffaceous horizon in the Wilyerpa Formation (Fm), just above the Appila (Sturtian) diamictite, provides a maximum age for the base of the interglacial sediments[2]. Overlying the Sturtian diamictite are two major coarsening-upward sequences. The lower Tapley Hill Fm siltstones grade upward into shallow marine sands, oolites and microbial reefs of the Etina Fm and northern equivalent (Balcanoona Fm).

The base of the Enorama Fm shales marks a major flooding surface that is followed by the second coarsening and shallowing-upward sequence, and culminates in the flake breccias, stromatolite bioherms, bioclastic packstones and oolitic grainstones of the Trezona Fm. Within the Enorama Fm shale lies an 18‰ negative shift in the $\delta^{13}C$ of inorganic carbon between the carbonates of the Etina ($\delta^{13}C = +8‰$) and Trezona Fms (Fig. 1c). This $\delta^{13}C$ excursion is the largest in Earth history. The interval of very negative $\delta^{13}C$ values just below the Elatina Fm (Marinoan) glacial deposits is called the Trezona anomaly. The Trezona anomaly has been linked to the initiation of ice-house conditions[3,4], and has been used to correlate overlying glacial deposits around the world[5,6]. The Elatina Fm and its Nuccaleena Fm cap dolostone have been correlated to U–Pb isotope-dilution thermal-ionization mass spectrometry (ID–TIMS) zircon-dated Marinoan successions in China[7] and Namibia[8] that are ~635 Myr old, with the contact between the two formations serving as the global boundary stratotype section and point for the base of the Ediacaran period (Fig. 1b).

Environmental setting and composition of bioclasts

One of the most common facies associations in the Trezona Fm of the central Flinders is stromatolite flake breccia and bioclast packstone filling the space between stromatolite heads (Fig. 2a,b) with up to one metre of synoptic relief[9]. The bioclast packstones also are found as dune-cross-stratified channel fill between larger stromatolite bioherms, and sheet-like overbank deposits. Over the course of mapping and measuring 14 detailed sections through the Trezona Fm (Fig. 1), we identified a great diversity of bioclasts. Most packstones contain clasts of probable microbial origin, such as spalled flakes of adjacent stromatolite laminae (Fig. 2b and Supplementary Fig. S1a,b) and ripped-up and rolled-up sediment with cohesion enhanced by the presence of microbial mats. However, many bioclasts have anvil, wishbone, ring and perforated slab morphologies (Fig. 2c–g) that are difficult to assign to an abiotic roll-up or bacterial mat origin. In addition, the red colour and calcite composition of these distinctively shaped clasts are unique to the packstones (and even packstone clasts entrained in the overlying Elatina Fm diamictite (Supplementary Fig. S1C) as far as 65 km from the nearest Trezona Fm stromatolite reef outcrop) and are not found *in situ* as layers elsewhere in the Trezona Fm that could have been brecciated and transported. Therefore, we suspect that the 1-cm-scale red bioclasts represent the remnants of a community of organisms endemic to the stromatolite-packstone environment.

In thin section, the packstone matrix is an interlocking network of equant calcite crystals and floating circular crystal aggregates (peloids) coated with a rim of variably thick micritic cement (Fig. 2h–j,o,p). Mixed in with the peloids are bulbous and chambered micritic textural elements (Fig. 2k,l) and rare coccoid spheroids composed of clay (and rarely Fe oxides and organic matter) and intergrown with calcite spar (Fig. 2n). The centimetre-scale, distinctively shaped bioclasts (red in outcrop) are

[1]Department of Geosciences, Princeton University, Princeton, New Jersey 08544, USA, [2]Situ Studio, 20 Jay Street #203, Brooklyn, New York 11201, USA, [3]Department of Paleobiology, MRC-121, Smithsonian Institution, PO Box 37012, Washington, District of Columbia 20013-7012, USA, [4]Princeton Institute for the Science and Technology of Materials, Princeton University, Princeton, New Jersey 08544, USA. *e-mail: maloof@princeton.edu.

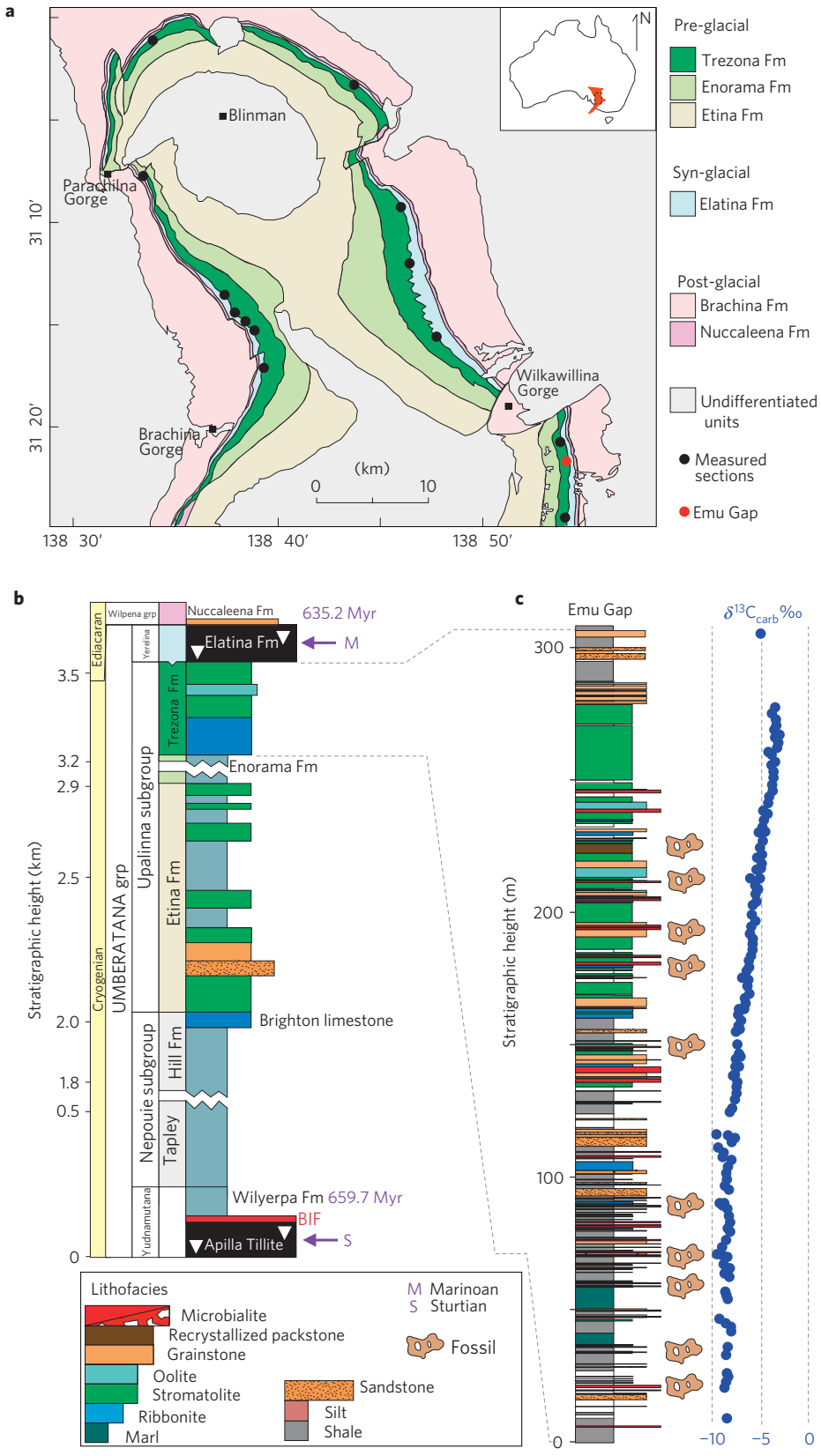

Figure 1 | Geological and stratigraphic setting of the Trezona Formation. a, Geological map of the central Flinders Ranges, with measured section locations marked by black and red dots. The Australia map inset locates the Adelaide Rift Complex in red and the central Flinders study region in the dashed black rectangle. **b**, Schematic stratigraphic section through the Cryogenian of South Australia. Note the changes in scale within the thick Tapley Hills and Enorama Fm siltstones. The 635.2 Myr age for the end of the Marinoan ice age comes from correlation to Namibia[8] and China[7]. The 659.7 Myr age for the Wilyerpa Fm comes from a section in the northern Flinders[2]. **c**, Detailed lithostratigraphy and $\delta^{13}C$ from Emu Gap, with labelled fossil horizons. Etina Fm carbonates have near-constant $\delta^{13}C$ values of +8‰ (ref. 45).

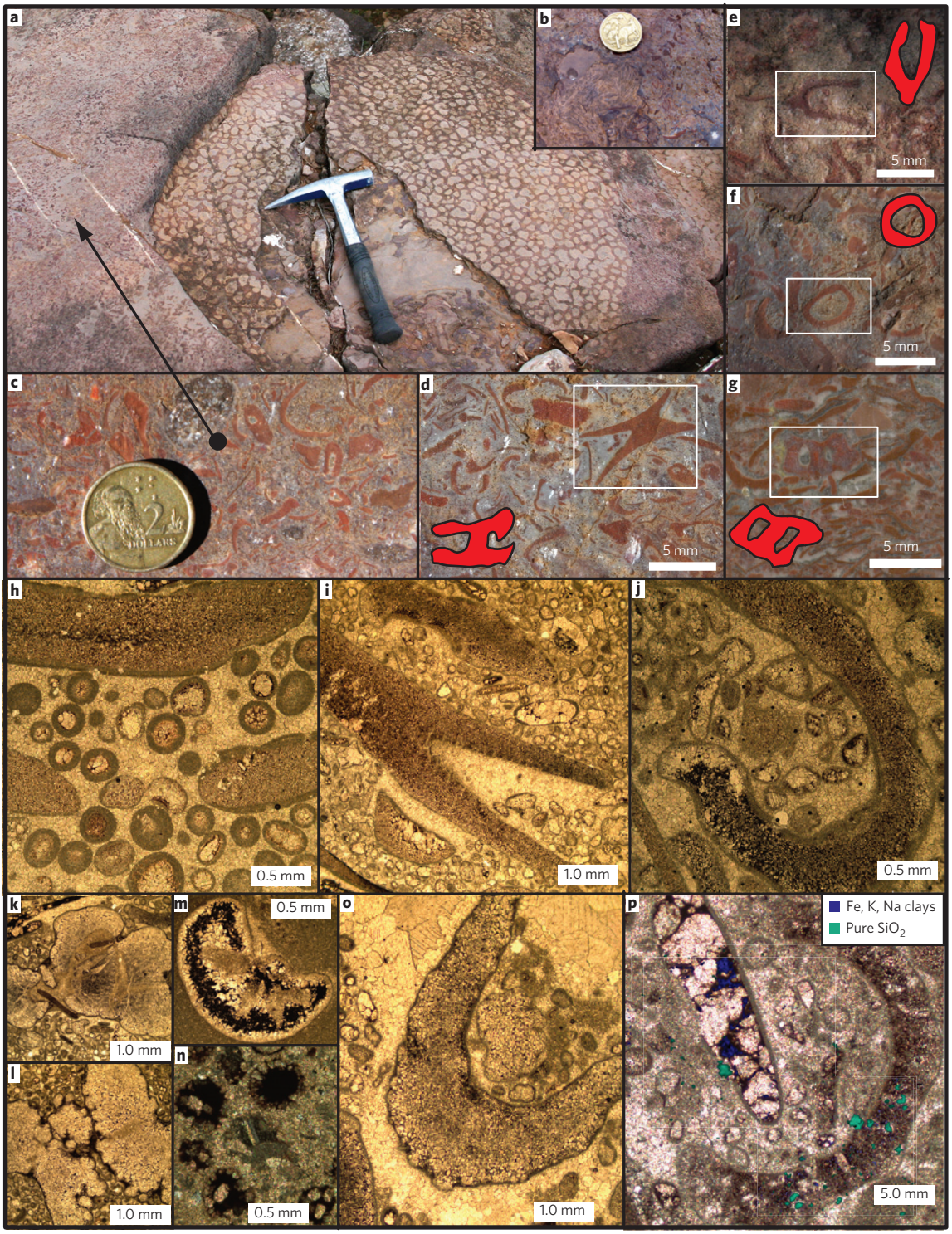

Figure 2 | Diverse morphology of the Trezona Formation fossils. a–**g**, Outcrop photographs from the Trezona Fm showing the range of skeletal morphologies in fossil debris onlapping and draping a stromatolite bioherm (under the hammer in **a**). **b** depicts tabular beige stromatolite flake breccia in the lower left mixing with distinctive red fossil debris in the upper right. For each 3D model presented in Fig. 3, we extracted 624 2D sections to compare to the common 2D sections apparent in outcrop (Supplementary Fig. S4). Common shapes in both outcrop (photos) and in 2D sections through the models (red objects) include anvils (**d**), wishbones (**e**), rings (**f**) and perforated slabs (**g**). **h**–**p**, Thin-section photomicrographs in plane polarized light. The matrix in all samples is composed of equant interlocking calcite crystals. Floating in the matrix are 0.1–0.5-mm-diameter spherical (**h**,**n**) and kidney-shaped (**m**) grains composed of crystalline calcite interiors with variable quantities of opaque clay, and extremely fine micritic calcite coatings (**h**). Bioclasts are a mix of opaque clays (dark blue in E-SEM EDXs element map overlay on transmitted and reflected light photomicrograph (in **p**)), 0.05–0.1 mm pure SiO_2 blebs (green in E-SEM EDXs overlay (in **p**)) and calcite crystals that sometimes coarsen towards the edges of the clasts (**j**). In general, wishbones tend to have the distinctive SiO_2 blebs (lower right of **p**), anvils contain more uniformly micro-crystalline calcite with disseminated SiO_2 and tabular flakes tend to have coarser calcite interiors with larger clay patches (upper left of **p**). Bioclast edges have micritic rims irrespective of the interior crystal size. **k** and **l** depict bulbous, chambered micro-textures similar to polymuds reported from other Neoproterozoic microbialites[37,38].

coated with micritic cement of uniform thickness (Fig. 2i,j,o,p). The interiors of the bioclasts are composed of calcite spar (usually finer than the matrix), and crystals sometimes decrease in size from the inner edge of the clast's micritic rim inward. We interpret the gradient in crystal size as heterogeneous cementation and recrystallization from the exterior of the clasts inward. However, the contact between micrite coating and mixed clay–chert–calcite interiors is usually sharp, with no evidence of diffusive or porosity-following micritization. In a few examples, spaced and isolated calcite spar is seen to grow from the rim coating towards the clast's interior (Fig. 2p), perhaps filling an aperture or perforation in the clast. Attenuated total reflectance Fourier transform infrared (ATR-FTIR) spectroscopic comparisons of powders prepared from matrix and bioclast material suggest that bioclasts are richer in either iron or manganese (Supplementary Fig. S2), perhaps explaining the red colour. Environmental scanning electron microscope (E-SEM) energy-dispersed X-ray system (EDXs) elemental mapping identifies Fe, Na, K clays forming irregular patches inside the most coarsely recrystallized and tabular-shaped clasts (Fig. 2p). In contrast, the best preserved wishbone-shaped bioclasts contain very finely disseminated Fe-rich clays and elliptical 0.1–0.5-mm-diameter chert blebs that are either interior to the bioclast or cross-cut the outer edge and micrite coating (Fig. 2p). We have not successfully documented any diagnostic microstructures or textures that identify the bioclasts as the weakly calcified organic walls of a specific macro-alga or animal, nor have we found specific evidence to interpret the chert blebs as biogenic silica.

Three-dimensional fossil reconstruction

Similar to the 1-cm-scale, goblet-shaped *Namacalathus* fossils (Supplementary Fig. S5) in packstones of the late Ediacaran in Namibia[10], the consistent scale and great abundance of a small number of distinctive shapes suggests that the Trezona Fm bioclasts represent different two-dimensional (2D) sections through a single fossil organism. To test this hypothesis, we construct 3D digital models of individual specimens from one block sample of packstone. Most 3D fossil reconstructions use computed tomography (CT) scanning technology and rely on X-rays to image significant density contrasts between organic matter and sediment in heterogeneous media. Our fossils, like many calcified organisms preserved in limestone of similar density, cannot be imaged with X-rays. Furthermore, the solubilities of the calcite fossils and matrix are similar enough that simple acid maceration is unsuccessful at liberating 3D fossil forms. Therefore, we apply a 3D fossil reconstruction routine that involves serial grinding and scanning at 50.8 μm intervals[10,11]. We develop a new routine to turn auto-traces of individual specimens into a point cloud that can be meshed and modelled as a 3D volume (Fig. 3). The new routine minimizes human interpretation and generates the model volume based entirely on colour contrast in the original digital photographs.

The 3D forms resulting from individual specimen reconstructions are not identical, but many reconstructions share a number of common features. The 3D objects are centimetre-scale, ellipsoidal and contain an interconnected network of 1-mm-diameter interior canals (Fig. 3). The models do not have consistent symmetry in external or internal topology. 2D sections (Supplementary Fig. S4) through the 3D models result in anvils, wishbones, horseshoes and perforated slabs, identical in morphology and scale to those observed in outcrop photographs (Fig. 2c–g). All of the canals (with one possible exception in Supplementary Fig. S3) connect to recessed apertures. At least three specimens have a very short tube-shaped appendage at the base that could be part of a stalk or holdfast. Although the weakly calcified organic walls seem to have been malleable and easily deformed during compaction, the consistent nearly circular cross-sections of the interior canals suggest that the topological asymmetry of these objects is primary.

Palaeobiological interpretation

These structures could be either casts of filaments or similar forms, or ripped-up flakes of microbial mat that were subsequently mined for organic matter by macroborers living at the sediment–water interface. The topology of the network and the recessed apertures are inconsistent with these structures being casts. The macroboring interpretation explains the texture and possibly the relatively clay-rich nature of clast interiors as relict bacterial mat, rather than the uniform sparry calcite expected to replace skeletons. However, it is not clear how both the exterior walls of the clasts and the interior walls of the tunnels would be coated with micrite of uniform thickness and texture. Also, the Trezona Fm tunnels are interconnected and always both enter and exit the clast—in other words, the tunnels do not dead-end like the borings of most endolithic organisms. No borings are found penetrating *in situ* stromatolites or microbialites.

Endolithic fungi and algae are common in coral reefs from Upper Devonian to recent times, but their borings tend to be much smaller (0.1–6 μm in diameter) than the Trezona Fm tunnels (1 mm; ref. 12). The oldest macroborers so far are reported from Lower Cambrian Archaeocyathid reefs in Labrador, where the borings are straight cylinders normal to the reef surface that do not branch or interconnect[13]. These borings are on average 2 cm long and 1 mm in diameter, and are thought to be made by polychaete or sipunculid worms[13]. The Trezona Fm canals would be significantly more complex and ~130 Myr older than the Labrador macroborers, and would be ~70 Myr older than large cnidarian-grade organisms of the Ediacaran.

Potential biologic affinities for these organisms include microbialites, giant protists, calcareous algae and metazoans. Algal nodules, thrombolites and stromatolites are common in the fossil record, but have laminar or columnar structures and lack the regular, internal canals and apertures found in the Trezona Fm forms. The Trezona Fm fauna is found as broken and transported bioclasts in channel fill between stromatolite bioherms, but both macro-algae and metazoans, such as sponges, could have thrived as sessile organisms near the bathymetric highs formed by stromatolites.

The formation of microbial carbonates is often facilitated by the microbial production of extracellular polymeric substances, which can act to stabilize and preserve microbial communities[14]. These may include channels and canal systems that provide nutrients and oxygen and remove wastes, but these canals are normally 20–40 μm wide[15], and the biofilms are generally <100 μm in height. None of these characteristics matches the Trezona Fm material.

Most unicellular eukaryotes are microscopic and lack cell–tissue specialization. However, giant (1–3 cm diameter), nearly spherical deep-sea protists from the Bahamas produce bilaterian-like sediment traces that prompted comparison to Proterozoic ichnofauna[16,17]. Calcified protists, such as foraminifera, may reach centimetre-scale and have complex camerate structures with internal spaces surrounded by walls[18]. Xenophyophores are large, complex, deep-sea dwelling protists that contain internal pores and build their skeletons out of polysaccharides and available debris (such as foram tests and sponge spicules) that could be calcified during diagenesis[19]. Protists, however, do not have the macroscopic internal canal networks and growth asymmetry seen in the Trezona Fm fossils.

Macro-algae such as *Grypania*[20,21] are present in the fossil record by 1.5 Gyr ago. Codiacean and dasycladalean green algae can make simple curved bioclasts and skeletons with internal pores[22]. However, algae have a complex internal anatomy with cylindrical pores that fall into several size classes, mostly much

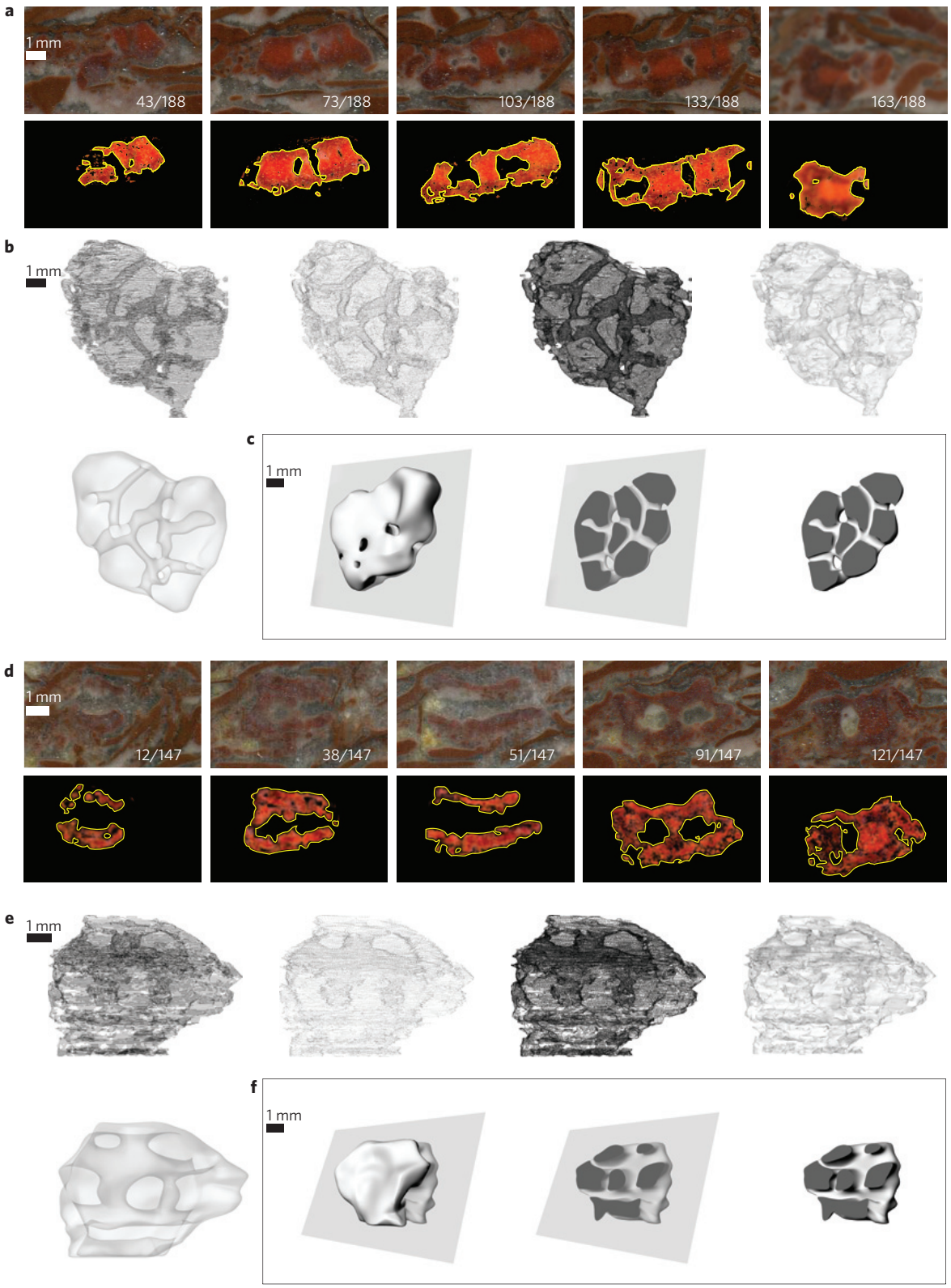

Figure 3 | Three-dimensional reconstruction of the Trezona Formation fossils. a–f, Digital models of two specimens (**a–c** and **d–f**). **a**,**d** illustrate the auto-trace (yellow lines) routine in 5 (of 188 and 147) serial images used to construct the model in **b**,**c** and **e**,**f**. The top panel of **a**,**d** contains raw images with white labels indicating the frame number of each section, and the bottom panel of **a**,**d** contains contrast-enhanced images with yellow autotraces. **b**,**e** depict, from left to right, the original auto-traced polygons arrayed in the third dimension, the polygons converted to a point cloud, the raw mesh derived from the point cloud, a semi-transparent 3D model volume of the mesh and a low-pass-filtered version of the semi-transparent model. **c**,**f** is a rendered depiction of the smooth model volume, then sliced perpendicular to the plane of the original traces in **a**,**d**. These specimens are asymmetric, both in its external form and internal canal network, although the canals are of uniform diameter. The specimens in **a–c** and **d–f** are representative of the external and internal topologies found in the best preserved fossils.

smaller than 1 mm. The oldest calcifying green macro-algae are reported from Ordovician–Silurian rocks[23,24]. Some red algae also form distinctly calcified walls[22] that have been confused with lower Palaeozoic chaetetid sponges[25,26]. Macroscopic, but non-calcifying, floridophyte red algae are found in the immediately post-Marinoan Doushantuo Fm of China[27]. However, the pores and columns in red algae are generally 30–50 μm in diameter, similar to the dimensions of the cells. Finally, an alga would have no reason to circulate water internally or to maximize internal surface area away from the chemical or radiative gradients it uses for an autotrophic metabolism.

Possible animal-body fossils in the pre-Marinoan

The Trezona Fm fossils share a number of characteristics with simple sponge-grade organisms, including the interconnected network of 1-mm-diameter canals entering and exiting the fossil through circular apertures. These structures could serve a clear function as part of the water canal system and filter-feeding apparatus of a simple sponge. In some instances, lone calcite spars grow inward from micritic rims (Fig. 2p), perhaps through primary orifices such as ostia. The least recrystallized wishbone specimens contain elliptical SiO_2 blebs that cross-cut clast walls and micrite coatings (Fig. 2p) and could be siliceous spicule roots, but we have not found unambiguous whole spicules attached to clasts or floating in the matrix. Although the Trezona Fm fossils are significantly smaller, and lack the hexactinellid spicule network and the prominent oscular disc, they do share some similarities in morphology with *Palaeophragmodictya*, which has been interpreted as 2D impressions of an Ediacaran-age sponge in coarse sandstone of the Rawnsley Quartzite from the Adelaide Rift Complex, South Australia[28]. In particular, the upper surface of *Palaeophragmodictya* is typically preserved as a series of intersecting grooves 2–3 mm in diameter that may represent infilled canals.

Were the Trezona Fm organisms primary biocalcifiers? The micrite of uniform thickness and texture coating both the exterior surface and the interior canal walls could represent weakly calcified cell layers sandwiching the mesohyl of a sponge-grade organism. However, texturally similar (but less uniform in thickness) micrite also coats peloids that do not seem to be part of the Trezona Fm organisms. Some form of very early partial cementation is required to maintain the circular cross-sections of the canals during transport and burial deformation. The Trezona Fm fossils could have been lightly mineralized by the precipitation of calcite on an organic template, as has been interpreted for late Ediacaran *Cloudina*[29] and *Namacalathus*[30], which are preserved as casts of void-filling calcite. Alternatively, the original organic skeletons could have been coated in a bacterial extracellular polymeric substance following their death. The chemical composition of the Fe, Na, K clays found in the Trezona Fm bioclasts is similar to that of authigenic minerals precipitated by microbial biofilms[31] during replacement of soft tissue[32]. The extracellular polymeric substance would also have formed a template for abiotic calcite precipitation[33].

The interconnected canal system and asymmetric body plan are the most powerful arguments for the sponge hypothesis. Textural, biocalcification and spicule arguments remain ambiguous in isolation, but together support the sponge hypothesis. There is an expectation that a simple tube should represent the simplest sponges[34], so the complicated network of canals seen in the Trezona Fm forms may not represent the oldest sponge-grade organisms.

The sponge interpretation is consistent with molecular-clock dates for the Eumetazoa–sponge divergence[35]. Lipid biomarkers suggestive of Demosponges have been found in strata below the Hadash Fm (Marinoan) cap carbonate in Oman[36]. Calcified chambered microfossil textures of millimetre scale and putative sponge affinity have also been reported from Etina-Fm-equivalent (Fig. 1b) microbialite reefs in the Gammon Ranges of South Australia[37] and the >723-Myr-old lower Little Dal Group reefs of the Mackenzie Mountains, Canada[38]. However, the Trezona Fm organisms are older than the oldest definitive body fossil evidence for animals[39] and the oldest putative sponge spicules[40] found in the Doushantuo Fm phosphorites of South China that lie above the cap carbonate to Marinoan glacial sediments (undisputed sponge spicules do not appear until the late Early Cambrian period[41], but see ref. 42). The realization that living sponges are probably paraphyletic indicates that topologies such as the water canal system are shared ancestral characteristics with other basal Metazoa, and probably with other now-extinct stem lineages[43]. Thus, the Trezona Fm organisms may be stem metazoans or members of an entirely extinct lineage. We conclude that, although Trezona Fm fossils do not share sufficient diagnostic synapomorphies with other clades to demonstrate phylogenetic affinity, several characteristics are best explained by a generalized sponge-grade metazoan.

If the Trezona Fm fauna is the first body-fossil evidence for the pre-Marinoan sponges predicted by molecular-clock and lipid-biomarker studies, then we are left with an interesting ecological puzzle. The first 30 Myr of the Ediacaran period were characterized by a diverse assemblage of microfossils but no apparent metazoans. The earliest probable metazoans, large soft-bodied organisms that lived in fairly deep-water siliciclastic environments and never found in association with carbonate reefs[44], do not appear until 579 Myr ago. Thus, there is a long gap between the Trezona Fm fossils and other animals fossils, and an even longer ecological gap until cnidarian-grade *Cloudina* and *Namacalathus* re-inhabit thrombolite reefs of the latest Ediacaran, ~90 Myr later[30].

Methods

We collected 32 block samples of bioclastic packstone from various stratigraphic levels in complete Trezona Fm sections around the central Flinders anticline (Fig. 1a). Variably oriented polished slabs and thin sections were prepared from each sample. We chose one 8.5 × 7.5 cm slab for serial grinding. That slab was cut into a cube, drilled with one registration hole in each corner, and mounted with epoxy in a shallow magnetic holder. Using a Kent Industries Model K08-250AHD precision surface grinder with a changeable 1 cm diamond wheel, we removed 50.8 μm of material and then scanned the surface to generate 470 serial images in a bitmapped format (a total of 23.9 mm).

We wrote a Matlab script to cross-correlate and precisely orient each image and create an aligned image stack. We then run a Visual Basic script that automates a series of consecutive operations in three different softwares. First, Adobe Photoshop applies a batch crop to zero-in on the fossil of interest, and a colour correction to homogenize colour contrast between images. Next, Adobe Illustrator establishes threshold red–green–blue values for the fossil and 'auto traces' each image to generate vector outlines of fossil shapes in each successive layer. Adobe Illustrator then batch exports the trace polylines in the dxf file format. Rhino converts the polylines to points and arrays them into the third dimension based on the 50.8 μm spacing between layers, thus establishing a 3D point cloud. Rhino runs a search algorithm, layer by layer, to remove outliers beyond a specified distance from the point cloud. This process serves as a low-pass filter. The 3D point cloud is converted to a triangulated mesh that can be rotated, sliced and analysed for quantities such as surface area, volume and porosity. Finally, a smooth 3D surface model is created using the subdivision modelling open-source software Blender. The point clouds described above are used as a scaffold when preparing these final models.

The entire process from image stack to digital 3D model takes approximately one hour per fossil. Our methodology is similar to that outlined in ref. 10. The disadvantage of our method is that it requires more proprietary software. The advantage of our method is that it is more adaptable to a range of object shapes, sizes and colour contrasts. For example, we were able to reproduce the *Namacalathus* models using the original imagery of ref. 10 (Supplementary Fig. S5).

The elemental analysis was carried out using a FEI Quanta 200 FEG E-SEM equipped with an integrated Oxford EDXs. The chemical information covering a wide range of elements was collected using a 15 keV electron probe from cross-section samples without any surface coating. Both Kα and Kβ lines were used for identification of various elements including Fe, Mn and so on.

Received 28 June 2010; accepted 9 July 2010; published online 17 August 2010

References

1. Preiss, W. in *The Adelaide Geosyncline of South Australia, Late Proterozoic Stratigraphy, Sedimentation, Palaeontology and Tectonics* Vol. 53 (ed. Preiss, W.) (Geological Survey of South Australia, 1987).
2. Fanning, C. M. *Geological Society of America Abstracts with Programs* Vol. 38, 115 (2006).
3. Schrag, D., Berner, R., Hoffman, P. & Halverson, G. On the initiation of a snowball Earth. *Geochem. Geophys. Geosyst.* **3,** 1036 (2002).
4. Pavlov, A., Hurtgen, M., Kasting, J. & Arthur, M. Methane-rich Proterozoic atmosphere. *Geology* **31,** 87–90 (2003).
5. Halverson, G., Maloof, A. & Hoffman, P. The Marinoan glaciation (Neoproterozoic) in northeast Svalbard. *Basin Res.* **16,** 297–324 (2004).
6. Halverson, G. *et al.* Toward a Neoproterozoic composite carbon-isotope record. *Geol. Soc. Am. Bull.* **117,** 1181–1207 (2005).
7. Condon, D. *et al.* U–Pb ages from the Neoproterozoic Doushantuo formation, China. *Science* **308,** 95–98 (2005).
8. Hoffmann, K-H., Condon, D., Bowring, S. & Crowley, J. A U–Pb zircon date from the Neoproterozoic Ghaub Formation, Namibia: Constraints on Marinoan glaciation. *Geology* **32,** 817–820 (2004).
9. Preiss, W. Palaeoecological interpretations of South Australian stromatolites. *J. Geol. Soc. South Aust.* **19,** 501–532 (1973).
10. Watters, W. & Grotzinger, J. Digital reconstruction of calcified early metazoans, terminal Proterozoic Nama Group, Namibia. *Paleobiology* **27,** 159–171 (2001).
11. Sutton, M., Briggs, D., Siveter, D. & Siveter, D. Methodologies for the visualization and reconstruction of three-dimensional fossils from the Silurian Herefordshire lagerstätte. *Palaeontol. Electron.* **4,** 1–17 (2001).
12. Bentis, C., Kaufman, L. & Golubic, S. Endolithic fungi in reef-building corals (order: Scleractinia) are common, cosmopolitan, and potentially pathogenic. *Biol. Bull.* **198,** 254–260 (2000).
13. James, N. & Kobluk, D. The oldest macroborers: Lower Cambrian of Labrador. *Science* **197,** 980–983 (1977).
14. Riding, R. Microbial carbonates: The geological record of calcified bacterial-algal mats and biofilms. *Sedimentology* **47** (suppl. 1), 179–214 (2000).
15. Lawrence, J., Korber, D., Hoyle, B., Casterton, J. & Caldwell, J. Optical sectioning of microbial biofilms. *J. Bacteriol.* **173,** 6558–6567 (1991).
16. Matz, M., Frank, T., Marshall, J., Widder, E. & Johnsen, S. Giant deep-sea protist produces bilaterian-like traces. *Curr. Biol.* **18,** 1849–1854 (2008a).
17. Bengston, S. & Rasmussen, B. New and ancient trace makers. *Science* **323,** 346–347 (2009).
18. Brusca, R. & Brusca, G. *Invertebrates* 2nd edn (Sinauer Associates, 2003).
19. Tendal, O. A monograph of the Xenophyophoria (Rhizopodea, Protozoa). *Galathea Rep.* **12,** 7–99 (1972).
20. Walter, M., Oehler, J. & Oehler, D. Megascopic algae 1,300 million years old from the Belt supergroup, Montana: A reinterpretation of Walcott's Helminthoidichnites. *J. Paleontol.* **50,** 872–881 (1976).
21. Han, T. & Runnegar, B. Megascopic eukaryotic algae from the 2.1-billion-year-old Negaunee iron-formation, Michigan. *Science* **257,** 232–235 (1992).
22. Wray, J. *Calcareous Algae* (Elsevier, 1977).
23. Laporte, L. Codiacean algae and algal stromatolites of the Manlius Limestone (Devonian) of New York. *J. Paleontol.* **37,** 643–647 (1963).
24. Mierzejewski, P. Ultrastructure, taxonomy and affinities of some Ordovician and Silurian microfossils. *Palaeontol. Pol.* **47,** 129–220 (1986).
25. Riding, R. Solenopora is a chaetetid sponge, not an alga. *Palaeontology* **47,** 117–122 (2004).
26. Brooke, C. & Riding, R. Ordovician and Silurian coralline red algae. *Lethaia* **31,** 185–195 (1998).
27. Xiao, S. *et al.* The Neoproterozoic Quruqtagh Group in eastern Chinese Tianshan: Evidence for a post-Marinoan glaciation. *Precambr. Res.* **130,** 1–26 (2004).
28. Gehling, J. & Rigby, J. Long expected sponges from the Neoproterozoic Ediacaran Fauna of South Australia. *J. Paleontol.* **70,** 185–195 (1996).
29. Grant, S. Shell structure and distribution of *Cloudina*, a potential index fossil for the terminal Proterozoic. *Am. J. Sci.* **290-A,** 261–294 (1990).
30. Grotzinger, J., Watters, W. & Knoll, A. Calcified metazoans in thrombolite–stromatolite reefs of the terminal Proterozoioc Nama Group, Namibia. *Paleobiology* **26,** 334–359 (2000).
31. Toporski, J. *et al.* Morphologic and spectral investigation of exceptionally well-preserved bacterial biofilms from the Oligocene Enspel formation, Germany. *Geochim. Cosmochim. Acta* **66,** 1773–1791 (2002).
32. Briggs, D. The role of decay and mineralization in the preservation of soft-bodied fossils. *Annu. Rev. Earth Planet. Sci.* **31,** 275–301 (2003).
33. Bosak, T. & Newman, D. Microbial nucleation of calcium carbonate in the Precambrian. *Geology* **31,** 577–580 (2003).
34. Manuel, M. Phylogeny and evolution of calcareous sponges. *Can. J. Zool.* **84,** 225–241 (2006).
35. Peterson, K., Cotton, J., Gehling, J. & Pisani, D. The Ediacaran emergence of bilaterians: Congruence between the genetic and the geological fossil records. *Phil. Trans. R. Soc. B* **363,** 1435–1443 (2008).
36. Love, G. *et al.* Fossil steroids record the appearance of Demospongiae during the Cryogenian. *Nature* **457,** 718–721 (2009).
37. Wallace, M. & Woon, E. *Selwyn Symposium, Vol. Abstract 91 of Neoproterozoic Climates Origin of Early Life* 17–21 (Geological Society of Australia Victoria Division, 2008).
38. Neuweiler, F., Turner, E. & Burdige, D. Early Neoproterozoic origin of the metazoan clade recorded in carbonate rock texture. *Geology* **37,** 475–478 (2009).
39. Xiao, S., Zhang, Y. & Knoll, A. Three-dimensional preservation of algae and animal embryos in a Neoproterozoic phosphorite. *Nature* **391,** 553–558 (1998).
40. Li, C., Chen, J. & Hua, T. Precambrian sponges with cellular structures. *Science* **279,** 879–882 (1998).
41. Bengston, S., Conway Morris, S., Cooper, B., Jell, P. & Runnegar, B. Early Cambrian fossils from South Australia. *Mem. Assoc. Aust. Palaeontol.* 1–364 (1990).
42. Sperling, E., Robinson, J., Pisani, D. & Peterson, K. Where's the glass? Biomarkers, molecular clocks, and microRNAs suggest a 200-Myr missing Precambrian fossil record of siliceous sponge spicules. *Geobiology* **8,** 24–36 (2010).
43. Sperling, E., Pisani, D. & Peterson, K. in *The Rise and Fall of the Ediacaran Biota,* Vol. 286 (eds Vickers-Rich, P. & Komarower, P.) 355–368 (Geol. Soc. Lond. Spec. Publ., 2007).
44. Xiao, S. & Laflamme, M. On the eve of animal radiation: Phylogeny, ecology, and evolution of the Ediacara biota. *Trends Ecol. Evol.* **24,** 31–40 (2009).
45. Swanson-Hysell, N. *et al.* Cryogenian glaciation and the onset of carbon-isotope decoupling. *Science* **328,** 608–611 (2010).

Acknowledgements

W. Watters provided us with example imagery, and, along with J. Hawthorne, gave us helpful Matlab advice. B. Evans allowed us to use his precision grinding machine at MIT, E. Feldman provided useful advice about machine design and machine code and S. Myneni helped us with the ATR-FTIR spectroscopy. We would like to thank B. E. Girit, W. A. Rozen, S. Briedfjord and A. Lukyanov of Situ Studio. B. Dyer, J. Strauss, N. Swanson-Hysell and N. Xu assisted with field work. S. Bowring, T. Duffy, J. Grotzinger, A. Knoll, M. Manuel, S. Porter, E. Sperling, G. Subsol and S. Xiao provided stimulating discussion. Flinders National Park and numerous pastoralists graciously allowed us to conduct field work on their land. The research was financially supported by NSF-EAR0842946 to A.C.M. and NSF-DMR-0819860 to the Princeton Center for Complex Materials.

Author contributions

A.C.M. and C.V.R. conducted the field work. C.V.R. carried out the serial grinding and imaging. R.B., B.M.S., C.V.R., C.C.C., F.J.S. and A.C.M. did the 3D modelling. G.R.P., N.Y., A.C.M. and C.V.R. did the E-SEM EDX analyses. C.V.R. conducted the ATR-FTIR spectroscopy. A.C.M. and D.H.E. wrote the paper.

Additional information

The authors declare no competing financial interests. Supplementary information accompanies this paper on www.nature.com/naturegeoscience. Reprints and permissions information is available online at http://npg.nature.com/reprintsandpermissions. Correspondence and requests for materials should be addressed to A.C.M.

PALAEONTOLOGY

Wringing out the oldest sponges

Evidence from biomarkers and molecular clocks points to the existence of sponges tens of millions of years before their earliest fossil remains. Fossils from South Australia may narrow that gap.

Marc Laflamme

In the first half of the Neoproterozoic era (1,000–542 million years (Myr) ago), the Earth experienced a tremendous upheaval. Amidst the build-up and eventual rifting of the supercontinent Rodinia, there is evidence for at least two global Snowball Earth glaciations, along with a shift in global ocean chemistry from sulphide-rich to iron-rich conditions and a dramatic rise in atmospheric oxygen concentrations[1]. These catastrophic changes were the backdrop to the evolution and eventual dominance of multicellular animals, which arguably represents the greatest biological revolution the Earth has seen. The earliest definitive signs of animal life first appeared in the latter half of the Ediacaran period (about 635 to 542 Myr ago)[2]. Although the Ediacaran is best known for unusual forms of life that bear little resemblance to biota found today[3,4], some of the oldest animal remains are those of the humble sea sponge[5]. Now, writing in *Nature Geoscience*, Maloof and colleagues[6] describe unusual fossils from rocks that pre-date the later Marinoan Snowball glaciation, which they interpret as the fossil remains of an early sponge.

Molecular clocks[7], which reflect rates of molecular change in DNA, and biomarker studies of sponge-specific organic compounds[8] both strongly indicate that sponges were present in the Cryogenian interval, between approximately 850 and 635 Myr ago. However, sponge-body fossils of this age are frustratingly absent from the fossil record. It is only in the Late Ediacaran that the first probable sponge fossils, *Paleophragmodictya*[5], make their appearance (Fig. 1).

Looking almost 90 Myr earlier, Maloof and colleagues[6] describe a series of peculiar fossils from the Trezona Formation of the Flinders Ranges of South Australia. These fossils are up to several millimetres in size and are present in various shapes such as circles, anvils, wishbones and rings. Maloof and colleagues used newly developed software to stitch together images of serially ground 50-micrometre-thick slices of the fossils into three-dimensional models. During this process, it was shown that the seemingly disparate fossils actually represented different slices through an irregularly shaped organism (Fig. 1, inset). Intriguingly, the reconstructions also highlight a series of interior chambers and canals that are about one millimetre in diameter. The authors interpret this chambered network as a primitive water-canal system typical of sponges. However, in the absence of other clearly identifiable sponge characteristics — such as the skeletal elements known as spicules, the inhalant porocyte canals, or the large excretory osculum opening — much of the evidence that the Trezona fossils are sponges relies on the interpretation of their functional morphology.

The lack of modern sponge characteristics in the Trezona fossils is a challenge to their interpretation. However, with each new discovery of a Precambrian animal, the rigid boundaries that have guided our classification of extant biota become more blurry. From a biological perspective, this is to be expected: the deeper in time we venture, the more likely we are to find stem taxa that hadn't yet evolved the shared derived characteristics that define the crown group. Of course, these shared characteristics must also be preserved in the fossil record, and we are only just beginning to unravel the processes that transform a living organism into a fossil. Balancing evolutionary processes and preservational biases to explain the absence of critical data in fossils is a fine tightrope to walk. Both of these processes can — and will — account for missing data in the fossil record, and it is certain that neither process is working in isolation. More importantly,

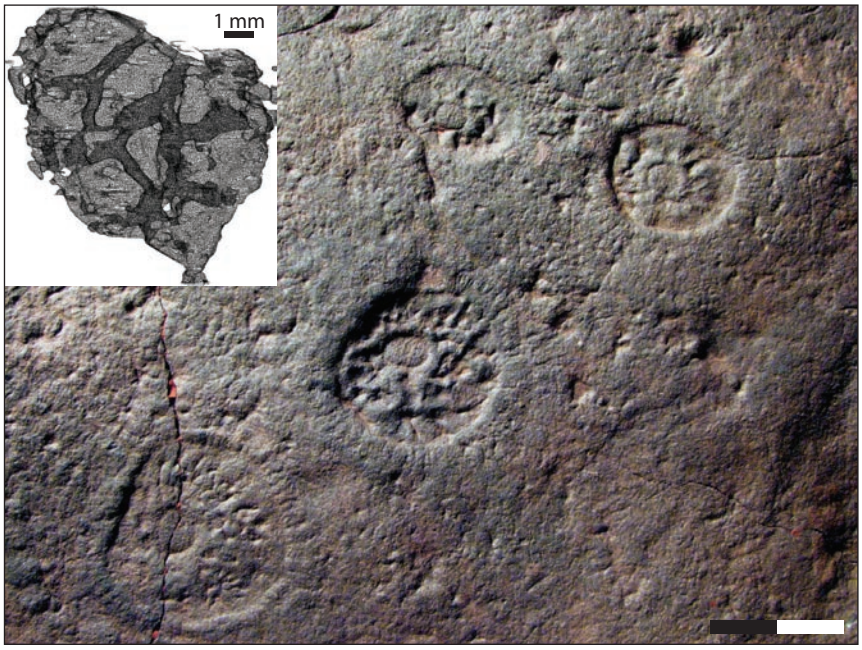

MARC LAFLAMME

Figure 1 | The earliest probable sponges include the Ediacaran *Paleophragmodictya* (SAM P32352A-F), found in the Flinders Ranges of South Australia. Maloof and colleagues[6] describe fossils from older sections in the Flinders Ranges (inset). These globular, asymmetric forms have unusually large networks of canals and are interpreted as the remains of primitive sponges that lived 90 Myr earlier than *Paleophragmodictya*. Scale bar: 2 cm.

the differentiation between a character having yet to evolve and one that has not been preserved shapes the construction of the topology of an evolutionary tree and can strongly bias evolutionary hypotheses[9,10].

In the case of primitive sponges, the debate centres primarily on the glaring absence of spicules from sediments before the Cambrian period[7,11], 542 Myr ago, and whether this absence represents an evolutionary or preservational issue. Modern sponge spicules are composed of either calcium carbonate or silica, which are structurally and developmentally distinct from one another[12]. These different types of spicule could be independently derived and therefore could represent a case of convergent evolution. This scenario allows for the possibility that spicules independently evolved at the beginning of the Cambrian, in response to an extrinsic factor such as predation.

On the other hand, it could be that spicules evolved much earlier and were not preserved in the fossil record until the conditions necessary for their fossilization were met[7]. Some of the Trezona fossils that underwent the least amount of alteration contain elliptical blebs of silica that, as Maloof and colleagues argue, might represent the roots of siliceous spicules. It remains unclear whether these silica blebs were formed by biological or diagenetic processes. Should they represent true spicule roots, it would go a long way towards suggesting that the lack of Cryogenian and Ediacaran sponge spicules may be a preservational bias.

As the search for ancient sponges continues, new palaeontological techniques and functional morphology studies, such as those presented by Maloof and colleagues[6], are likely to be instrumental in uncovering the roots of early animal evolution. ❐

Marc Laflamme is in the Department of Geology and Geophysics, Yale University, New Haven, Connecticut 06520, USA.
e-mail: marc.laflamme@yale.edu

References

1. Knoll, A. H. *Life on a Young Planet: The First Three Billion Years of Evolution on Earth* (Princeton Univ. Press, 2003).
2. Xiao, S. & Laflamme, M. *Trends Ecol. Evol.* **24,** 31–40 (2009).
3. Narbonne, G. M. *Science* **305,** 1141–1144 (2004).
4. Narbonne, G. M. *et al. J. Paleontol.* **83,** 503–523 (2009).
5. Gehling, J. G. & Rigby, J. K. *J. Paleontol.* **70,** 185–195 (1996).
6. Maloof, A. *et al. Nature Geosci.* doi:10.1038/ngeo934 (2010).
7. Sperling, E. A. *et al. Geobiol.* **8,** 24–36 (2010).
8. Love, G. D. *et al. Nature* **457,** 718–721 (2009).
9. Donoghue, P. C. J. & Purnell, M. A. *BioEssays* **31,** 178–189 (2009).
10. Sansom, R. A. *et al.* Nature **463,** 797–800 (2010).
11. Yin L. *et al. Chinese Sci. Bull.* **46,** 1828–1832 (2001).
12. Brusca, R. C. & Brusca, G. J. *Invertebrates* 2nd edn (Sinauer Associates, 2002).

Published online: 17 August 2010